Optimization of Advanced Square Wave AC-GTAW Parameters to Improve Localized Corrosion Resistance of AA6082-T651 Aluminum Welds

Mohammad Tabeahmadi [1], Reza Dehmolaei [2,*], Seyed Reza Alavi Zaree [2]

[1] M.Sc. Student, Department of Material Science and Engineering, Shahid Chamran University of Ahvaz, Ahvaz, Iran
[2] Ph.D. assistant professor, Department of Material Science and Engineering, Shahid Chamran University of Ahvaz, Ahvaz, Iran

ARTICLE INFO

Article history:

Received 30 July 2020
Accepted 12 September 2020
Available online 15 September 2020

Keywords:

AA6082-T651 alloy
Advanced square wave AC-GTAW
Localized corrosion
Taguchi method
Analysis of variance(ANOVA)
Regression method

ABSTRACT

In this study, optimization of advanced square wave alternative current GTAW(ASW-AC-GTAW) parameters were conducted to improve localized corrosion resistance of AA6082-T651 aluminum alloy welds. To this objective, positive half cycle current(PHC), negative half cycle current(NHC), frequency(F) and positive half cycle current percentage(PHC%) were selected as main welding parameters and altered at three levels according to Taguchi method and $L_9(3^4)$ orthogonal array. To study the localized corrosion resistance of weld metals; potentiodynamic polarization test was performed on all samples and corresponding $\Delta E_{pit}(E_{pit} - E_{corr})(mV)$ were measured and considered as evaluation criterion. Implementation of variance analysis(ANOVA) on measured data and S/N (Signal-to-Noise) ratios indicated that the optimum levels of PHC, NHC, F, and PHC% were 300A, 190A, 2Hz, 40%, respectively. According to ANOVA of S/N ratios, contribution of PHC, NHC, F, and PHC% to the results were 35.05%, 25.98%, 23.57%, and 15.27%, consecutively. Interval domain for average ΔE_{pit} calculated with 95% confidence level to be (379.4 , 386.54) (mV). confirmation sample was welded under optimum condition. The values of ΔE_{pit} of optimum sample were 381.13 and 385.47 mV. Both of this measurement fallen in the Interval domain. Therefore, the experimental results were in excellent agreement with analytical predictions. The regression model for predicting ΔE_{pit} values was obtained using multivariate nonlinear regression.

1-Introduction

Aluminum alloys have gathered a great deal of application in different industries due to their versatile properties. AA6082-T651 alloy is used extensively in different applications such as aerospace, marine, transportation industries, cryogenics and coastal conditions due to the properties such as high specific strength, good weldability, corrosion resistance, formability and low cost [1–5]. Strengthening of AA6082-T651 occurs through heat treatment and artificial aging that causes the formation of Mg_2Si precipitations in aluminum matrix [6–8]. This alloy is typically fusion welded with GTAW and GMAW processes[9,10]. 5000 aluminum filler metals such as ER5356 are used

* Corresponding author:
E-mail address: Dehmolaei@scu.ac.ir

to reduce the solidification cracking sensitivity of AA6082-T651 joints [11]. Welding heat cycles cause many metallurgical changes in metals including dissolution of precipitates, grain growth, alteration of mechanical and corrosion properties[12]. The microstructure of ER5356 weld metal consists of columnar α-Al dendrites, discontinuous interdendritic network which is identified as Al-Mg_2Al_3 eutectic, and secondary phases distributed throughout the matrix. It has been revealed that the interdendritc region contains Al, Mg, Si, Mn and Fe elements, while the secondary phases are identified as Mg_2Al_3, Mg_5Al_8, and $Al_{12}(Fe.Mn)_3Si$ [11,13,14]. Considering the chemical composition of base metal and filler metal, the formation of β'' ، β' and Q precipitates in weld zone are possible [15]. Differences between the corrosion potential of the microstructural constituents, result in reduction of resistance to pitting and intergranular corrosion [16–18]. Resistance to localized corrosion will become a major priority when using AA6082-T651 in marine welded structures like ships and supporting structures of offshore oil platforms which are exposed to the environments containing chloride ions(Cl^-). [17,19,20].

In ASW-AC-GTAW process, the welding current fluctuates instantaneously between positive and negative half cycles at a certain frequency (i.e. pulsing current). This changes the convection patterns and creates vibration in the weld pool, that results in improvement of joint microstructure and properties. The process includes positive half cycle current (PHC), Negative half cycle current (NHC), frequency (F) and positive half cycle percentage (PHC% or balance) as the main parameters. Bear in mind that the thermal efficiency of PHCs (0.5) are less than NHCs (0.75), thus NHCs melt the base metals and create the weld pool while PHCs maintain an stable arc and provides oxide removal [9,21–23]. Reported metallurgical advantages of welding with pulsing current include weld zone grain refinement, segregation control, reduced solidification cracking sensitivity, less residual stresses and distortion [24–26].

Extensive researches were done on pulse current effects on joint mechanical properties [24–28]. However, despite of using AA6082-T651 welded structures in marine corrode media and the differences between weld metal and base metal corrosion resistant to pitting, less attention have been payed to weldments corrosion properties [16]. Moreover, the process parameters effect weld metal corrosion properties. Hence, The present research has been executed to comprehend the effects of ASW-AC-GTAW parameters on pitting corrosion of AA6082-T651 alloy welds.

Taguchi method as a systematic approach for experiment design and data analysis is used to control and improve product quality. Furthermore, the experiment design using Taguchi method reduces required tests, experiment cost and time. Optimization of ASW-AC-GTAW parameters using Taguchi method can result in weld quality improvement [16,29,30]. In this work, the experiment design carried out using $L_9(3^4)$ orthogonal array in accordance with Tguchi method.

2- Experimental Procedure

In this study, wrought AA6082-T651 alloy plates (150×100×6 mm) and ER5356 filler metal (2.4mm in diameter for root pass, 3.2mm in diameter for cap pass) were used. Nominal composition of AA6082-T651 alloy and ER5356 filler are presented in Table 1. Prior to welding procedure, cleaning and oxide removal of the specimens and filler metals were performed by HNO_3 and $NaOH$ chemical solutions. Schematic of joint design is presented in Fig. 1. Welding carried out by Miller Syncrowave 350 LX TIG machine with 16.8 V voltage and advanced square wave AC current (Fig. 2). The Scheme of the polarization test and the results evaluation process are shown in Fig 2 as well. High purity argon gas(99.9%) with 12 lit/min flow rate were used as shielding gas. The main parameters of ASW-AC-GTAW process and their levels are presented in Table 2.

Table 1. Chemical composition of base metal and filler metal (wt.%).

	Mg	Si	Cu	Mn	Fe	Ti	Cr	Zn	Al
AA6082 (base material)	0.6-1.2	0.7-1.3	0.25	0.4-1	0.50	0.10	0.25	0.20	Balance
ER5356 (filler metal)	4.5-5.5	0.25	0.1	0.05-0.20	0.40	0.06-0.20	0.05-0.20	0.10	Balance

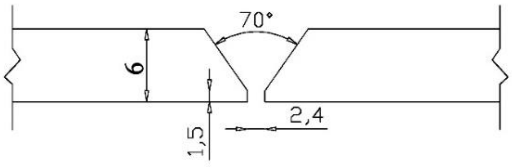

all dimensions are in mm

Fig. 1. Schematic of Joint design and dimensions.

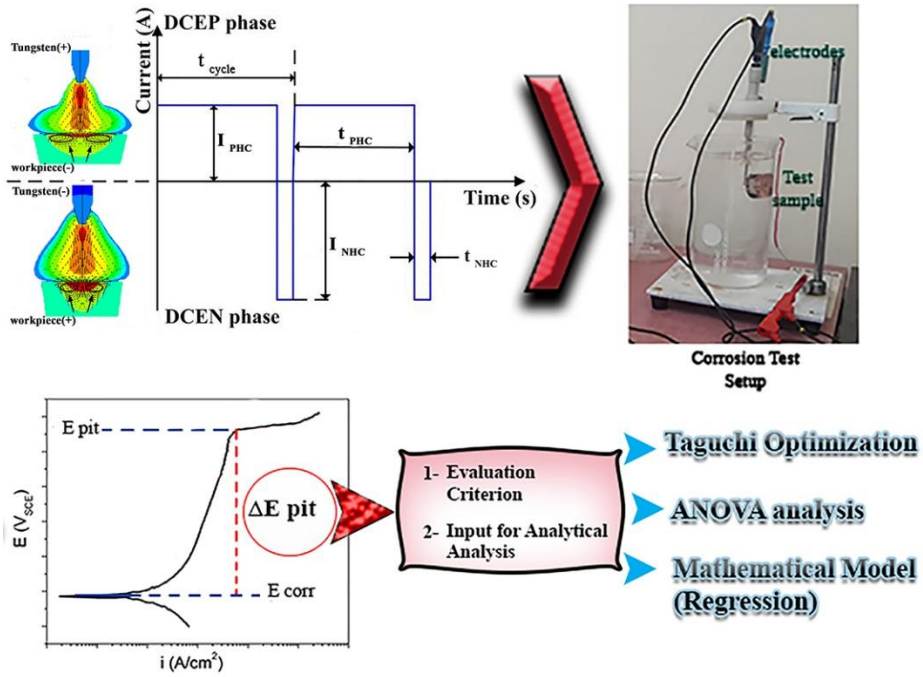

Fig. 2. schematic of current wave form in ASW-AC-GTAW process [9], scheme of the polarization test and results evaluation process.

Table 2. ASW-AC-GTAW variable parameters and levels of each parameter.

Parameters	**Abbr.**	**Levels**		
		1	2	3
Positive half cycle current (A)	PHC	300	280	260
Negative half cycle current (A)	NHC	170	190	210
Frequency (Hz)	F	2	6	10
Positive half cycle %	PHC%	40	60	80

Two specimens were cut off from each welded joint. The root of each weld was notched and a wire connection was fitted closely in the notched area. Specimens were mounted and sanded up to 3000 grid abrasive papers, then they were cleaned completely in an ultrasonic bath. Afterwards, the surface of each sample was masked with a nonconductive coating to obtain an exposure area about 25 mm^2. Each test was carried out in a cell containing 1 liter of 3.5 wt.% NaCl solution. The three electrode system was employed for conducting potentiodynamic polarization test with the test sample working as an anode, platinum rode as counter electrode and Ag/AgCl as a reference electrode. The Initial and final potential were consecutively -300 and +600 mV with respect to open circuit potential (E_{OCP}). Scanning rate was set to 0.5 mV/s , and due to the unstable nature of the E_{OCP} of this alloy, the test samples were kept in the cell for 1 h before starting the polarization tests to obtain steady measurements. $\Delta E_{pit}(mV)$ was measured and considered as evaluation criteria.

$$\Delta E_{pit} = E_{pit} - E_{corr} \quad (1)$$

Where $\Delta E_{pit}(mV)$, E_{pit} and E_{corr} are the width

of the passive region, pitting potential and corrosion potential, respectively.

Taguchi method and $L_9(3^4)$ orthogonal array (Table 3) were used to design the experiment. This array produces 9 welding combinations in which the four main welding parameters of ASW-AC-GTAW are varied in 3 levels. Compared to full factorial design which require 81 samples, using this method reduces the sample size, time and experimental costs. In order to decrease undesirable and uncontrollable variables (i.e. noise effects and bias data) workpieces were welded randomly according to the experiment design in the same day[16,31].

3- Results and discussion

3-1- polarization test

The results of polarization test for 18 samples are presented in table 4 and are plotted in Fig.3. The sample 7 with $\Delta E_{pit} = 98.829\, mV$ and sample 1 with $\Delta E_{pit} = 347.614\, mV$ exhibited the lowest and the highest mean of passive region, respectively. Other samples had an intermediate mean width of ΔE_{pit} ranging from 157.508 to 276.158 mV.

Table 3. $L_9(3^4)$ Orthogonal array – parameter combinations used for welding each joint (coded).

Joint no.	PHC level	NHC level	F level	PHC% level	Combinations (PHC,NHC,F,PHC%)
1	300	170	2	40	(1,1,1,1)
2	300	190	6	60	(1,2,2,2)
3	300	210	10	80	(1,3,3,3)
4	280	170	10	80	(2,1,3,3)
5	280	190	6	60	(2,2,2,2)
6	280	210	2	40	(2,3,1,1)
7	260	170	10	60	(3,1,3,2)
8	260	190	2	80	(3,2,1,3)
9	260	210	6	40	(3,3,2,1)

Table 4. Polarization test results (i.e. $\Delta E_{pit}(mV)$), MSD and S/N ratios corresponding to each joint no.

Joint no.	Combinations (PHC,NHC,F,PHC%)	$\Delta E_{pit}(1)$ (mV)	$\Delta E_{pit}(2)$ (mV)	Mean ΔE_{pit}(mV)	MSD	S/N ratio
1	(1,1,1,1)	345.69	349.53	347.61	8.28E-06	50.82
2	(1,2,2,2)	267.96	264.65	266.31	1.41E-05	48.51
3	(1,3,3,3)	156.48	158.55	157.52	4.03E-05	43.95
4	(2,1,3,3)	240.37	273.96	239.17	1.74E-05	47.57
5	(2,2,2,2)	248	250.86	249.43	1.60E-05	47.94
6	(2,3,1,1)	190.350	193.46	191.91	2.71E-05	45.66
7	(3,1,3,2)	96.39	101.26	98.83	1.03E-04	39.89
8	(3,2,1,3)	277.66	276.65	276.16	1.31E-05	48.82
9	(3,3,2,1)	157.76	159.53	158.65	3.97E-05	44.01

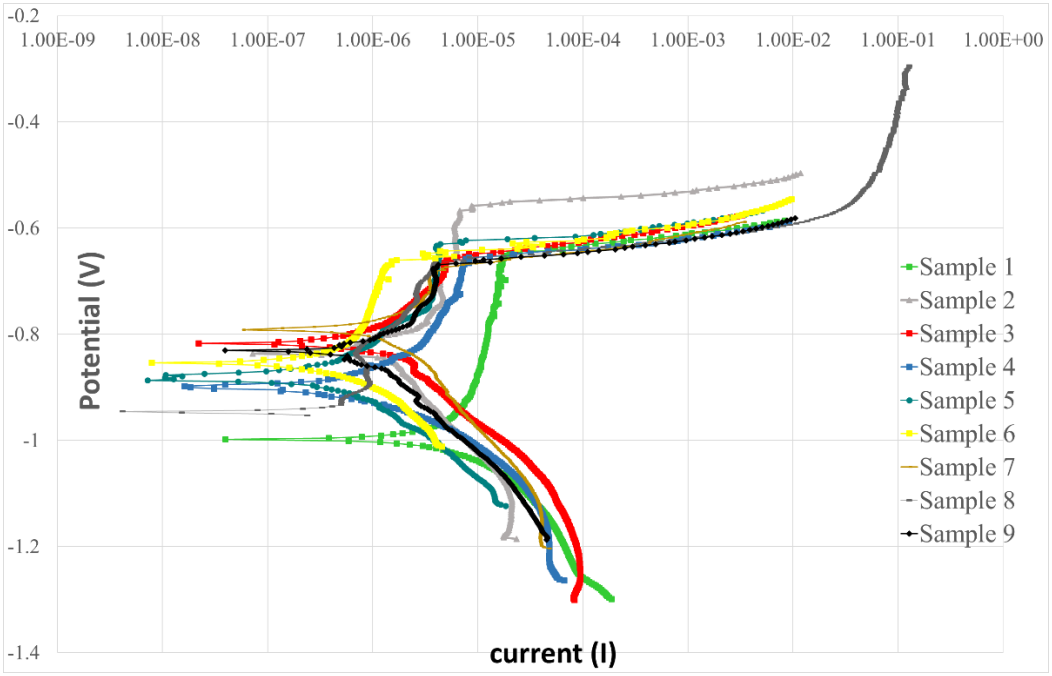

Fig. 3. Plot of Tafel polarization test results for 9 welded samples.

3-2- Finding the optimum condition

The highest width of passive region is desirable, and an increase in ΔE_{pit} means higher pitting corrosion resistance [32]. Therefore, in order to find out the optimum condition, analysis of data using Taguchi method on the average of ΔE_{pit} were carried out. For Taguchi method The "Larger The Better (LTB)" were used as quality control criterion. comparing the mean values is The usual method for data comparison, but it is not well suited when the objective is the performance consistency. Taguchi defines quality as the performance consistency, so a quantity called mean square deviation (MSD) were presented in order to measure it [16, 31]. MSD depends on quality control criterion and for the LTB, it is defined by the following equation[33]:

$$MSD=(1/n)\times\sum_{i=1}^{n}(1/y_i^2) \quad (2)$$

Where y_i is the result of ith sample (in present study ΔE_{pit} value of ith sample) and n is the number of test repetitions or replications (i.e. 2 in this case). Logarithmic transformation of the MSD called signal-to-noise (S/N) recommended by Taguchi for results evaluation [31,33]:

$$S/N = -10\log(MSD) \quad (3)$$

The average of ΔE_{pit} for 2 replications and corresponding MSDs and S/N ratios are given in Table 4. Average value of ΔE_{pit} corresponding to each level of the parameters are given in Table 5 and Fig 4. The average value of S/N ratios corresponding to each level of the parameters are given in Table 6 and Fig 5. Also, the quantity called $\Delta = Max - Min$ is presented in Tables 6, which ranks the parameters according to their influence on the obtained results. Considering the Δ of Taguchi analysis, welding parameters ranked as following: F (1st), NHC (2nd), PHC(3rd), PHC% (4th). Analysis of means declare that, if samples are welded in optimal condition (i.e. (PHC, NHC, F, PHC %) = (1,2,1,1)) , so the average of ΔE_{pit} for such samples would be maximum. Meanwhile, analysis of S/N ratios declare that, if samples are welded in optimal condition, so the steadiest performance could be expected. Noted that optimal combination did not exist in prior 9 welded samples that is not unusual because only 9 of 81 possible combinations were welded according to DOE.

Table 5. Mean analysis results.

parameters	$\overline{\Delta E_{pit,\ level\ 1}}$	$\overline{\Delta E_{pit,\ level\ 2}}$	$\overline{\Delta E_{pit,\ level\ 3}}$	optimum level (coded)	Optimum level (value)
PHC	**257.15**	226.84	177.88	1	300
NHC	228.54	**263.97**	169.36	2	190
F	**271.89**	221.38	168.59	1	2
PHC%	**251.89**	185.68	224.28	1	40%

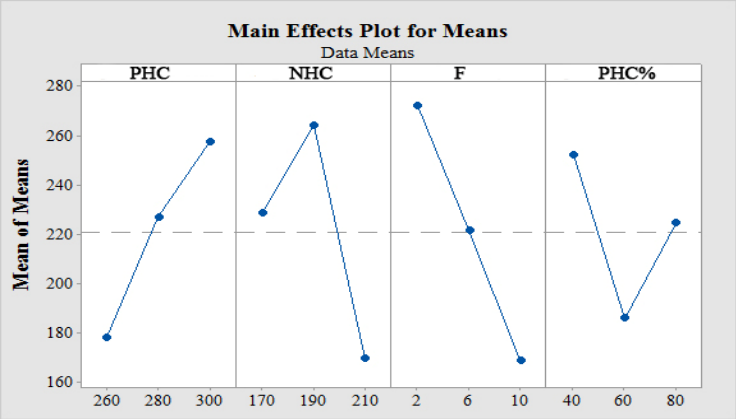

Fig. 4. Plot of Mean $\Delta E_{pit}(mV)$ of each parameter at three levels (i.e. Main effects plot for means).

Table 6. Mean S/N ratio analysis.

parameters	$\overline{(S/N)_{level\ 1}}$	$\overline{(S/N)_{level\ 2}}$	$\overline{(S/N)_{level\ 3}}$	optimum level (coded)	Optimum level (value)	Δ	rank
PHC	**47.76**	47.05	44.24	1	300	3.52	3
NHC	46.09	**48.42**	44.54	2	190	3.88	2
F	**48.43**	46.69	43.92	1	2	4.51	1
PHC%	**47.59**	44.68	46.78	1	40%	2.91	4

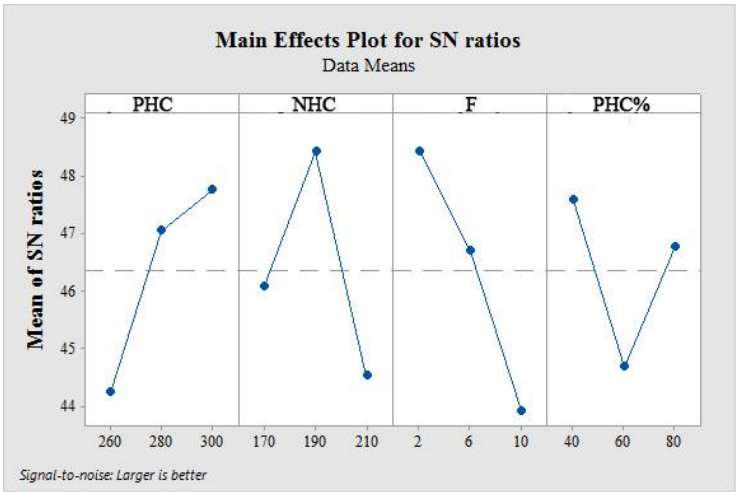

Fig. 5. Plot of Mean S/N ratios of each parameter at three levels (i.e. Main effects plot for S/N ratios).

3-3- Analysis of variance (ANOVA)

The Δ quantity ranked main parameters from the most influential parameter (F) to the least influential parameter (PHC %). But contribution of each parameter to the results should be determined. Hence, ANOVA was performed on $\overline{\Delta E_{pit}}$s (Standard ANOVA) and S/N ratios (ANOVA of S/N ratios). Both analyses are quite similar and terms of ANOVA were calculated through equations 5 to 9

[30,34]:

$$SS_T = \sum_i^m \eta_i^2 - (1/m) \times [\sum_{i=1}^m \eta_i]^2 \quad (5)$$

Where SS_T represents total sum of squares, m is total number of tests (in this case 18), η_i is S/N ratio (for ANOVA of S/N ratios) or ΔE_{pit} (for Standard ANOVA) of the i th test.

$$SS_P = \sum_{j=1}^t (S_{\eta_j}{}^2/t) - (1/m) \times [\sum_{i=1}^m \eta_i]^2 \quad (6)$$

Where *SSp* is the sum of squares from the tested parameters, *p* one of the tested parameters, *j* the level number of the p parameter, *t* the repetition of each level of the p parameter, and S_{η_j} the sum of S/N ratios (for ANOVA of S/N ratios) or $\overline{\Delta E_{pit}}$s (for Standard ANOVA) involving this parameter and level j.

$$V_p(\%) = (SS_p/D_p) \times 100 \quad (7)$$

Here V_p represents the variance of a tested parameter and D_p is the degree of freedom (DOF) of p parameter.

$$SS_p' = SS_p - D_p V_e \quad (8)$$

Where SS_p' is the corrected sum of squares for p parameter, and V_e represents the error variance.

$$P_p(\%) = (SS_p'/SS_T) \times 100 \quad (9)$$

Where P_p is the contribution percentage of p parameter to the obtained results.

The Results of standard ANOVA are given in Tables 7, Fig.6. The Results of ANOVA of S/N ratios are given in Tables 8, Fig.7 In accordance with ANOVA of S/N ratios, the contribution of F, NHC, PHC and PHC% to the results were 35.05%, 25.98%, 23.57%, and 15.27%, consecutively. According to standard ANOVA, the contribution of F, NHC, PHC and PHC% to the results were 34.81%, 29.80%, 20.87%, and 14.43%, respectively.

Table 7. Results of standard ANOVA table (i.e. ANOVA performed on ΔE_{pit}).

parameters	Degree of freedom (f)	Sum of squares (SS_P)	Variance (V)	F-ratio	pure sum of squares (SS_p')	Influence percentage (p)
PHC	2	19197.9	9598.95	1927.94	19187.94	20.87
NHC	2	27415.4	13707.7	2753.18	27405.44	29.80
F	2	32018.2	16009.1	3215.41	32008.24	34.81
PHC%	2	13274.3	6637.15	1333.06	13264.34	14.43
Error	9	44.8	4.98			0.09
Total	17	91950.6				100

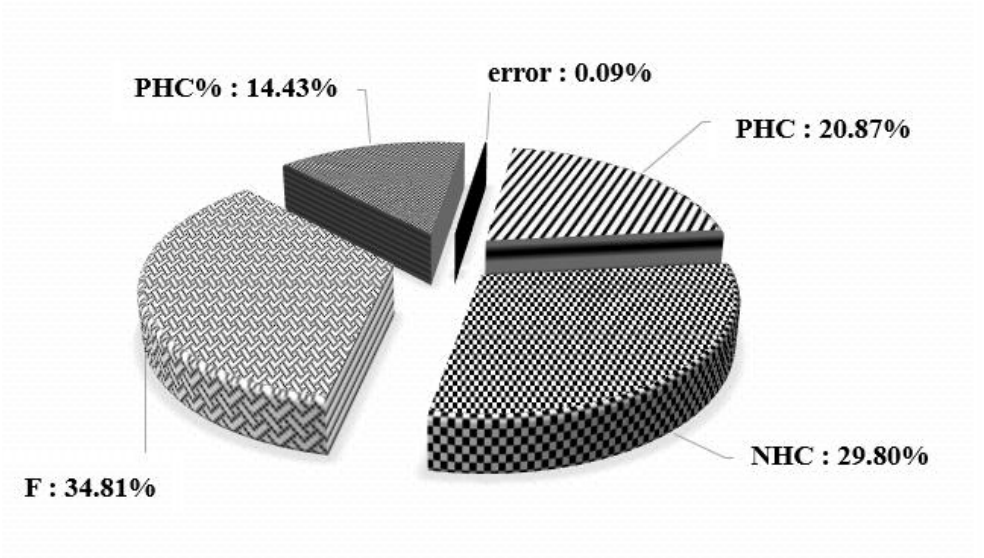

Fig. 6. Contribution diagram of main welding parameters to the results according to ANOVA of S/N ratios.

Table 8. Results of ANOVA performed on S/N ratio.

parameters	Degree of freedom (f)	Sum of squares (SS_P)	Variance (V)	F-ratio	pure sum of squares (SS'_p)	Influence percentage (p)
PHC	2	20.81	10.40	…	20.81	23.57
NHC	2	22.93	11.46	…	22.93	25.98
F	2	31.05	15.52	…	31.05	35.05
PHC%	2	13.47	6.73	…	13.47	15.27
Error	0	…	…	…	…	…
Total	8	91950.6				100

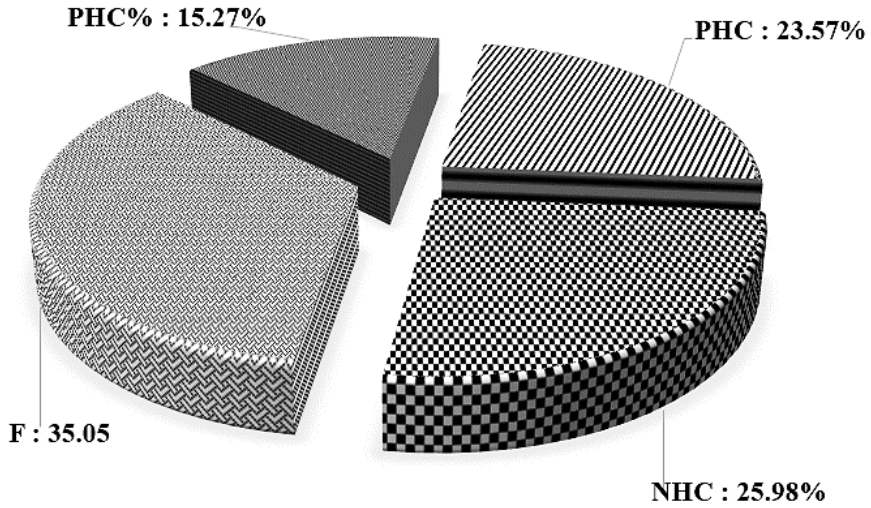

Fig. 7. Contribution diagram of main welding parameters to the results according to standard ANOVA.

3-4- F-Test (test of significance)

Identifying the significant parameters was accomplished by performing significance test on ANOVA data. In this regard, the F-ratio (V_P/V_e) calculated from experimental results is compared with the F-value obtained from the standard F-table for the desired confidence level(C.L.), risk and the degree of freedom of error (f_e). If the experimentally calculated F-ratio exceeds F-value extracted from the F-table, then the parameter is significant [31]. From table 8, PHC% has the least value of SS_P, which means the least contribution to the results. Experimentally calculated F-ratio for this parameter is 1333.6 while F-value extracted from the F-table for 95% confidence level, risk (α)=(1-C.L.)/100=0.05 and $f_e = 9$ is $F_{0.05}(1,9)95\% = 5.1174$ [31]. Therefore, this parameter passed the test of significance. Since the parameter with the least contribution to the result is significant then the rest of the parameters are significant too. For ANOVA of S/N ratios it can be seen that f_e is zero, therefore the F-ratio cannot be calculated and F-test is not applicable. Since the confidence level is 95%, so any parameters which contributed more than 5% to the results can be considered as a significant parameter [31].

3-5- Estimation of $\overline{\Delta E_{pit}}$ of optimal sample

The Following Taguchi model based on results average was used to estimate mean ΔE_{pit} for the optimum sample [16]:

$$\Delta E_{pit,\ estimated} = M\beta(M) + (\overline{\Delta E}_{pit,F_1} - M)\beta(F) + (\overline{\Delta E}_{pit,NHC_2} - M)\beta(NHC) + (\overline{\Delta E}_{pit,PHC_1} - M)\beta(PHC) + (\overline{\Delta E}_{pit,PHC\%_1} - M)\beta(PHC\%) \quad (10)$$

Where $\Delta E_{pit.estimated}$ is *mean* ΔE_{pit} estimated by Taguchi model, M is the total average of ΔE_{pit} of 18 tested samples and $\beta(M), \beta(F), \beta(NHC), \beta(PHC)$ and $\beta(PHC\%)$ are the coefficients corresponding to each parameter which can be calculated by the following equations [16]:

$$\beta(A) = 1 - (1/F_p) \quad (11)$$

$$\beta(M) = 1 - (V_e / \sum_i^m \eta_i^2) \quad (12)$$

Where F_p is experimentally calculated F-ratio of p parameter, $\sum_i^m \eta_i^2$ is the sum square of results. By replacing $\sum_i^m \eta_i^2$ =968,074 and V_e=4.98 in equation (12) gives $\beta(M) = 0.99995$. Using equation (10) and replacing the values from table 5 gives $\overline{\Delta E_{pit,\ estimated}}$ of optimal sample equal to 382.97 mV.

Prediction of the $\overline{S/N}$ ratio for the optimal condition was done by using equation (13) [30]:

$$(S/N)_{prediction} = (S/N)_m + \sum_{i=1}^{n}((S/N)_i - (S/N)_m) \quad (13)$$

Where $(S/N)_m$ is the average of S/N ratios, $(S/N)_i$ is the mean S/N ratio at the optimal level, and n is the number of the significant parameters. Using equation (13) and replacing the values presented in Table 6 in equation (13) gives $\overline{(S/N)_{prediction}}$ of optimal sample equal to 53.14. According to predicted S/N, $\overline{\Delta E_{pit}}$ of optimal sample is $\Delta E_{pit.\ prediction} = 454.26\ mV$. Hence, a wide range estimation of $\overline{\Delta E_{pit}}$ of optimal sample is obtained. Since the predicted values are mean ΔE_{pit} of optimal sample, then there is a 50/50 chance that the results of testing the optimal sample fall below or above the predicted value.

3-6- Finding confidence interval(C.I.)

The confidence interval (C.I.) is calculated as follows[31]:

$$C.I. = \pm\sqrt{F_\alpha(1,f_e)\times V_e / N_{eff}} \quad (14)$$

Where N_{eff} is the effective sample size or effective number of replications and calculated by the following expression:

$$N_{eff} = N/(1+\sum_p (f_p \times \beta(p))) \quad (15)$$

Where $\beta(p)$ is the β-factor of p factor. C.I. represents the boundaries of the expected performance in the optimum condition at a confidence level used for the F value from the standard F-table. For 95% C.L., F-value extracted from the standard F-table is $F_{0.05}(1,9)95\% = 5.1174$. By replacing $N_{eff} = 2$ and V_e=4.98 the confidence interval can be calculated as C.I. = ±3.57 mV. Therefore, the interval domain for average ΔE_{pit} of optimum sample calculated with 95% confidence level is expected to be (379.4 , 386.54) (mV). This domain means for a population of samples welded at the optimum condition, it can be expected that the $\overline{\Delta E_{pit}}$ of such set would be in the range between 379.4 and 386.54 mV. As the C.I. is calculated at 95% confidence level, then if many sets were welded at optimum condition and C.I. for each set were calculated, it can be expected that about 95% of these C.I.s would finally contain the mean ΔE_{pit} of such sets. As f_e is zero in ANOVA of S/N ratios, then V_e cannot be calculated and therefor, C.I. cannot be calculated either.

In order to confirm the results obtained from Taguchi and ANOVA, a sample was welded at the optimum condition (PHC, NHC, F, PHC%) = (1,2,1,1). Polarization test was performed two times for the optimum sample. The ΔE_{pit} values of the optimum sample were 381.13 and 385.47 mV. Both of these measurements were in the C.I. domain. Therefore, the experimental results were in excellent agreement with analytical predictions.

3-7- Finding regression model

Finding an empirical relation between the ASW-AC-GTAW parameters and the data obtained from polarization test (i.e. ΔE_{pit} values) was carried out using a multivariate nonlinear regression model. The simplest relation between the ASW-AC-GTAW parameters and ΔE_{pit} values can be described by the following equation:

$$y = \Delta E_{pit} = f(PHC,NHC,F,PHC\%) = f(x_1,x_2,x_3,x_4) \quad (16)$$

Where y is a substitute for ΔE_{pit} and x_1, x_2, x_3 and x_4 are substituted for PHC, NHC, F and PHC%, consecutively. To describe the more detailed relation between the main parameters of the process (i.e. independent variables) and ΔE_{pit} values (i.e. dependent variable) the following multivariate nonlinear equation was used:

$$y = y_0 + a\times x_1 + b\times x_1^2 + c\times x_2 + d\times x_2^2 + m\times x_3 + n\times x_3^2 + r\times x_4 + t\times x_4^2 \quad (17)$$

Where y_0 is the free term of regression eq. (17), the coefficients (a, c, m and r) are coefficients of linear terms and the coefficients (b, d, n and t) are coefficients of quadratic terms. The Coefficients of the regression model were calculated using SigmaPlot software. The following complete regression model has been obtained by replacing the values of each coefficient in the regression eq. (17):

$$y = -9445.1236 + 14.7939\times x_1 - 0.0229\times x_1^2 + 90.5012\times x_2 - 0.2460\times x_2^2 + 20.0566\times x_3 - 2.1319\times x_3^2 - 33.2839\times x_4 + 0.2717\times x_4^2 \quad (18)$$

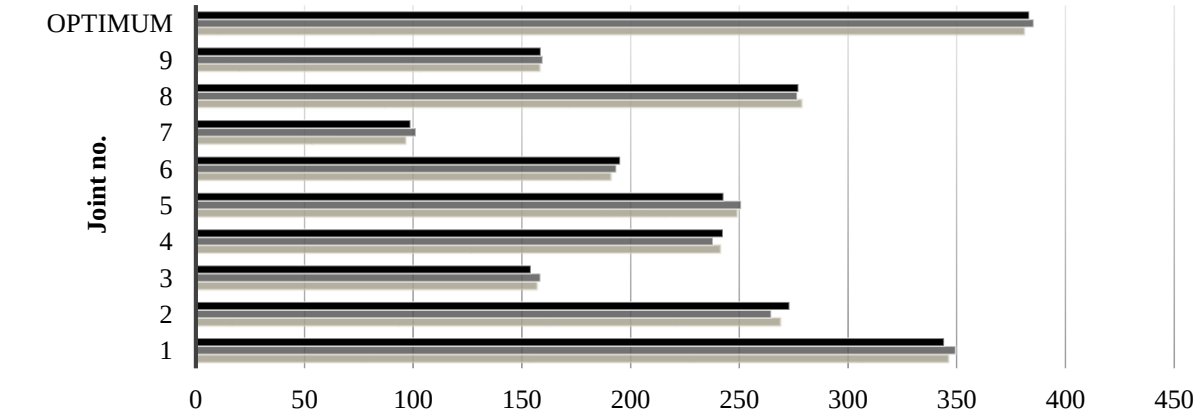

	1	2	3	4	5	6	7	8	9	Optimum
prediction	344.25	273.02	154.15	242.52	242.71	195.26	98.82	277.15	158.64	383.3
test 2	349.53	264.65	158.55	237.96	250.86	193.46	101.26	276.65	159.53	385.47
test 1	345.69	267.96	156.48	240.37	248	190.35	96.38	277.66	157.76	381.13

Fig. 8. Comparison between experimental data and predicted values obtained using regression model.

Table 9. ANOVA results of the regression model.

	Degree of Freedom(DF)	Sum of Squares(SS)	Mean Square (MS)	F statistic	P value
regression	8	139433.0913	17429.1364	597.4001	< 0.0001
residuals	11	320.9248	29.1750		
total	19	139754.0161	7355.4745		

Fitting of the regression model was evaluated by ANOVA. ANOVA results of the regression model were presented in Table 9. The comparison between experimental data and predicted values obtained using regression model are presented in Fig. 8.

If in ANOVA of the regression model, the value of F statistic is a large number it can be concluded that the independent variables contribute to the prediction of the dependent variable, and if the F ratio is around 1, it can be concluded that there is no association between the variables. The P value is the probability of being wrong in concluding that there is an association between the dependent and independent variables. The smaller the P value, the greater the probability, so that there is an association. Traditionally, it can be concluded that the independent variable can be used to predict the dependent variable when $P < 0.05$ [35]. From table 9 it can be seen that the value of F statistic is 597.4001 and the P value is less than 0.0001. The multiple correlation coefficient (R) and the coefficient of determination (R^2) and the adjusted R^2 (R^2_{adj}) are the measures of how well the regression model describes the data. R, R^2 and R^2_{adj} values near 1 indicate that the equation is a good description of the relation between the independent and dependent variables[36]. For the presented regression model R, R^2 and R^2_{adj} values were 0.9989, 0.9977 and 0.9960 respectively, and the standard error of estimation was 5.40. Therefore, it can be concluded that the regression model estimations are in excellent agreement with empirical data.

4- Conclusion

This study was conducted to optimize ASW-AC-GTAW parameters to improve localized corrosion resistance of AA6082-T651 Aluminum welds made by ER5356 filler metal. Experiment design was carried out using Taguchi method and $L_9(3^4)$ orthogonal array. The following conclusion can be drawn:

All parameters concluded in the experimental

design passed the F-test and proved to be significant parameters. Optimum condition obtained in accordance with Taguchi and mean analysis was (PHC, NHC, F, PHC%) = (1,2,1,1) (i.e. 300A, 190A, 2Hz and 40% respectively). According to ANOVA of S/N, F with 35.05% had the predominant contribution to the result, and NHC and PHC with 25.98%, 23.57% consecutively had an intermediate contribution to the result, and PHC% with 15.27% had the least contribution. The experiment error due to uncontrollable factors was about 0.09%. The confidence interval at 95% confidence level was between 379.4 and 386.54 mV. ΔE_{pit} values of the optimum sample were 381.13 and 385.47 mV which is in excellent agreement with analytical predictions. For the presented multivariate nonlinear regression model R, R^2 and R^2_{adj} values were 0.9989, 0.9977 and 0.9960 respectively, and the standard error of estimation was 5.40. Therefore, it could be concluded that Taguchi method , ANOVA and nonlinear regression are useful tools for optimization of ASW-AC-GTAW process and prediction of results.

References

[1] Z. Sekulski, Multi-objective topology and size optimization of high-speed vehicle-passenger catamaran structure by genetic algorithm, Mar. Struct. 23 (2010) 405–433. doi:10.1016/j.marstruc.2010.10.001.

[2] C. Vargel, M. Jacques, M.P. Schmidt, Corrosion of Aluminium, Elsevier Ltd., 2004. doi:10.1016/B978-008044495-6/50012-4.

[3] D.H. Park, S.W. Choi, J.H. Kim, J.M. Lee, Cryogenic mechanical behavior of 5000- and 6000-series aluminum alloys: Issues on application to offshore plants, Cryogenics (Guildf). 68 (2015) 44–58. doi:10.1016/j.cryogenics.2015.02.001.

[4] R. Manti, D.K. Dwivedi, A. Agarwal, Pulse TIG welding of two Al-Mg-Si alloys, J. Mater. Eng. Perform. 17 (2008) 667–673. doi:10.1007/s11665-008-9210-z.

[5] Y. Ruan, X.M. Qiu, W.B. Gong, D.Q. Sun, Y.P. Li, Mechanical properties and microstructures of 6082-T6 joint welded by twin wire metal inert gas arc welding with the SiO2 flux, Mater. Des. 35 (2012) 20–24. doi:10.1016/j.matdes.2011.09.002.

[6] C.D. Marioara, S.J. Andersen, J. Jansen, H.W. Zandbergen, The influence of temperature and storage time at RT on nucleation of the β" phase in a 6082 Al-Mg-Si alloy, Acta Mater. 51 (2003) 789–796. doi:10.1016/S1359-6454(02)00470-6.

[7] V. Noseda Grau, A. Cuniberti, A. Tolley, V. Castro Riglos, M. Stipcich, Solute clustering behavior between 293K and 373K in a 6082 Aluminum alloy, J. Alloys Compd. 684 (2016) 481–487. doi:10.1016/j.jallcom.2016.05.197.

[8] Abbas Bahrami, Modeling of Precipitation Sequence and Ageing Kinetics in Al-Mg-Si Alloys, This research was performed in the department of Materials Science and Engineering of Technical University of Delft., 2012. doi:10.1007/s13398-014-0173-7.2.

[9] J. Pan, S. Hu, L. Yang, D. Wang, Investigation of molten pool behavior and weld bead formation in VP-GTAW by numerical modelling, Mater. Des. 111 (2016) 600–607. doi:10.1016/j.matdes.2016.09.022.

[10] A. Kumar, P. Shailesh, S. Sundarrajan, Optimization of magnetic arc oscillation process parameters on mechanical properties of AA 5456 Aluminum alloy weldments, Mater. Des. 29 (2008) 1904–1913. doi:10.1016/j.matdes.2008.04.044.

[11] N. Kishore Babu, M.K. Talari, P. Dayou, S. Zheng, W. Jun, K. SivaPrasad, Influence of titanium-boron additions on grain refinement of AA6082 gas tungsten arc welds, Mater. Des. 40 (2012) 467–475. doi:10.1016/j.matdes.2012.03.056.

[12] V. Fahimpour, S.K. Sadrnezhaad, F. Karimzadeh, Corrosion behavior of aluminum 6061 alloy joined by friction stir welding and gas tungsten arc welding methods, Mater. Des. 39 (2012) 329–333. doi:10.1016/j.matdes.2012.02.043.

[13] K. Blommedal, Corrosion Development in Welded AA6082 Alloys, Norwegian University of Science and Technology, 2013.

[14] F.K. Mutombo, CORROSION FATIGUE BEHAVIOUR OF 5083-H111 AND 6061-T651 ALUMINIUM ALLOY WELDS, University of Pretoria, 2011.

[15] R. Braun, Nd:YAG laser butt welding of AA6013 using silicon and magnesium containing filler powders, Mater. Sci. Eng. A. 426 (2006) 250–262. doi:10.1016/j.msea.2006.04.033.

[16] E. Rastkerdar, M. Shamanian, A. Saatchi, Taguchi optimization of pulsed current GTA welding parameters for improved corrosion resistance of 5083 aluminum welds, J.

Mater. Eng. Perform. 22 (2013) 1149–1160. doi:10.1007/s11665-012-0346-5.
[17] F.E.-S. Hosni Ezuber, A. El-Houd, A study on the corrosion behavior of aluminum alloys in seawater, Mater. Des. 29 (2008) 802–805. doi:10.1016/j.matdes.2007.01.021.
[18] J.F. Li, Z.Q. Zheng, S.C. Li, W.J. Chen, W.D. Ren, X.S. Zhao, Simulation study on function mechanism of some precipitates in localized corrosion of Al alloys, Corros. Sci. 49 (2007) 2436–2449. doi:10.1016/j.corsci.2006.12.002.
[19] P.M. Natishan, W.E. O'Grady, Chloride Ion Interactions with Oxide-Covered Aluminum Leading to Pitting Corrosion: A Review, J. Electrochem. Soc. 161 (2014) C421–C432. doi:10.1149/2.1011409jes.
[20] V.S. Sinyavskii, V.D. Kalinin, Marine corrosion and protection of aluminum alloys according to their composition and structure, Prot. Met. 41 (2005) 317–328. doi:10.1007/s11124-005-0046-8.
[21] J.C. Dutra, L.M. Cirino, R.H. Gonçalves e Silva, AC–GTAW of aluminium – new perspective for evaluation of role of positive polarity time, Sci. Technol. Weld. Join. 15 (2010) 632–637. doi:10.1179/136217110X12813393169570.
[22] J. Pan, S. Hu, L. Yang, H. Li, Simulation and analysis of heat transfer and fluid flow characteristics of variable polarity GTAW process based on a tungsten-arc-specimen coupled model, Int. J. Heat Mass Transf. 96 (2016) 346–352. doi:10.1016/j.ijheatmasstransfer.2016.01.014.
[23] C.L. Jenney, A. O'Brien, Welding handbook, 1991. doi:10.1017/CBO9781107415324.004.
[24] T. Senthil Kumar, V. Balasubramanian, M.Y. Sanavullah, Influences of pulsed current tungsten inert gas welding parameters on the tensile properties of AA 6061 aluminium alloy, Mater. Des. 28 (2007) 2080–2092. doi:10.1016/j.matdes.2006.05.027.
[25] A. Hadadzadeh, M.M. Ghaznavi, A.H. Kokabi, The effect of gas tungsten arc welding and pulsed-gas tungsten arc welding processes' parameters on the heat affected zone-softening behavior of strain-hardened Al-6.7Mg alloy, Mater. Des. 55 (2014) 335–342. doi:10.1016/j.matdes.2013.09.061.
[26] M. Manikandan, M. Nageswara Rao, R. Ramanujam, D. Ramkumar, N. Arivazhagan, G.M. Reddy, Optimization of the Pulsed Current Gas Tungsten Arc welding process parameters for alloy C-276 using the Taguchi method, Procedia Eng. 97 (2014) 767–774. doi:10.1016/j.proeng.2014.12.307.
[27] S. BABU, T.S. KUMAR, V. BALASUBRAMANIAN, Optimizing pulsed current gas tungsten arc welding parameters of AA6061 aluminium alloy using Hooke and Jeeves algorithm, Trans. Nonferrous Met. Soc. China (English Ed. 18 (2008) 1028–1036. doi:10.1016/S1003-6326(08)60176-4.
[28] V. Rajkumar, N. Arivazhagan, Role of pulsed current on metallurgical and mechanical properties of dissimilar metal gas tungsten arc welding of maraging steel to low alloy steel, Mater. Des. 63 (2014) 69–82. doi:10.1016/j.matdes.2014.05.055.
[29] K. Nandagopal, C. Kailasanathan, Analysis of mechanical properties and optimization of gas tungsten Arc welding (GTAW) parameters on dissimilar metal titanium (6Al-4V) and aluminium 7075 by Taguchi and ANOVA techniques, J. Alloys Compd. 682 (2016) 503–516. doi:10.1016/j.jallcom.2016.05.006.
[30] M. Yousefieh, M. Shamanian, A. Saatchi, Optimization of the pulsed current gas tungsten arc welding (PCGTAW) parameters for corrosion resistance of super duplex stainless steel (UNS S32760) welds using the Taguchi method, J. Alloys Compd. 509 (2011) 782–788. doi:10.1016/j.jallcom.2010.09.087.
[31] R.K. Roy, A PRIMER ON THE TAGUCHI METHOD, second, Society of Manufacturing Engineers, 2010.
[32] E. Ghali, Corrosion Resistance of Aluminum and Magnesium Alloys Understanding, Performance, and Testing, John Wiley & Sons, Inc., 2010.
[33] G. Taguchi, S. Chowdhury, Y. Wu, Taguchi's Quality Engineering Handbook, ohn Wiley & Sons, Inc., 2005.
[34] M. Arivarasu, K. Devendranath Ramkumar, N. Arivazhagan, Comparative studies of high and low frequency pulsing on the aspect ratio of weld bead in gas tungsten arc welded AISI 304L Plates, Procedia Eng. 97 (2014) 871–880. doi:10.1016/j.proeng.2014.12.362.
[35] S. Weisberg, Applied Linear Regression, Third Edit, John Wiley & Sons, Inc., 2005. doi:10.2307/1269895.
[36] C. Aldrich, Exploratory analysis of metallurgical process data with neural networks and related methods, First edit, Elsevier Science B.V, 2002.